Protein destabilization and loss of protein-protein interaction are fundamental mechanisms in cblA-type methylmalonic aciduria

Plessl, Tanja ; Bürer, Céline ; Lutz, Seraina ; Yue, Wyatt W ; Baumgartner, Matthias R ; Froese, D Sean

Abstract: Mutations in the human MMAA gene cause the metabolic disorder cblA-type methylmalonic aciduria (MMA), although knowledge of the mechanism of dysfunction remains lacking. MMAA regulates the incorporation of the cofactor adenosylcobalamin (AdoCbl), generated from the MMAB adenosyltransferase, into the destination enzyme methylmalonyl-CoA mutase (MUT). This function of MMAA depends on its GTPase activity, which is stimulated by an interaction with MUT. Here, we present 67 new patients with cblA-type MMA, identifying 19 novel mutations. We biochemically investigated how missense mutations in MMAA in 22 patients lead to disease. About a third confer instability to the recombinant protein in bacterial and human expression systems. All 15 purified mutant proteins demonstrated wild-type like intrinsic GTPase activity and only one (p.Asp292Val), where the mutation is in the GTP binding domain, revealed decreased GTP binding. However, all mutations strongly decreased functional association with MUT by reducing GTPase activity stimulation upon incubation with MUT, while nine mutant proteins additionally lost the ability to physically bind MUT. Finally, all mutations interfered with gating the transfer of AdoCbl from MMAB to MUT. This work suggests loss of functional interaction between MMAA and MUT as a disease-causing mechanism that impacts processing and assembly of a cofactor to its destination enzyme.

DOI: https://doi.org/10.1002/humu.23251

Protein destabilization and loss of protein-protein interaction are fundamental mechanisms in *cblA*-type methylmalonic aciduria

Supplementary Information

Tanja Plessl[1,3] , Céline Bürer[1], Seraina Lutz[1], Wyatt W. Yue[2], Matthias R. Baumgartner[1, 3,4#], D. Sean Froese[1, 4#]

[1]Division of Metabolism and Children's Research Center, University Children's Hospital, CH-8032 Zurich, Switzerland

[2]Structural Genomics Consortium, Nuffield Department of Clinical Medicine, University of Oxford, Oxford OX3 7DQ, United Kingdom

[3]Zurich Center for Integrative Human Physiology, University of Zurich, Switzerland

[4]radiz – Rare Disease Initiative Zurich, Clinical Research Priority Program for Rare Diseases, University of Zurich, Switzerland

#To whom correspondence may be addressed:

M.R.B.

Division of Metabolism and Children's Research Center, University Children's Hospital, Steinwiesstrasse 75, CH-8032 Zurich, Switzerland

Tel: +41 (0)44 266 7722

Fax: +41 (0)44 266 7167

Email: matthias.baumgartner@kispi.uzh.ch

D.S.F

Tel: +41 (0)44 266 7156

Email: sean.froese@kispi.uzh.ch

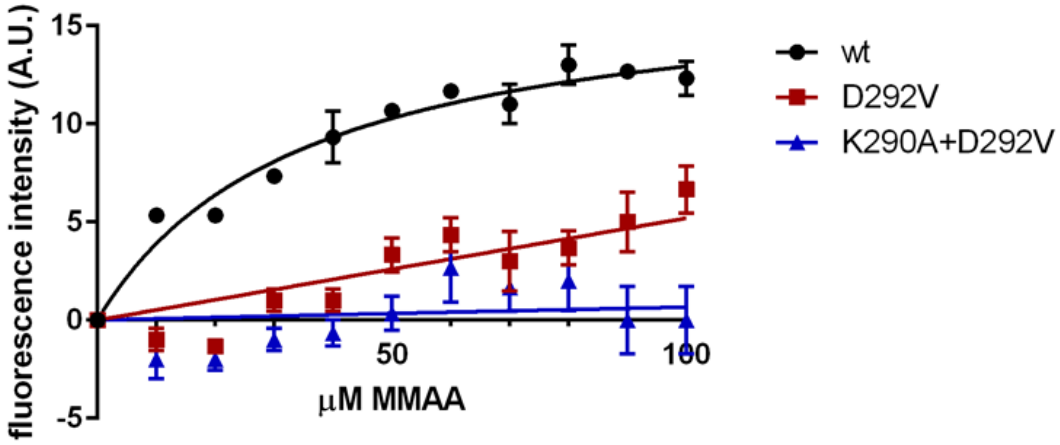

Supp. Figure S1. Mant-GTP binding to wt MMAA or MMAA mutants. Binding of GTP to MMAA was measured by titration of wt MMAA or mutants (10-110 μM) to 10 μM mant-GTP. Mant-GTP binding was measured as change in fluorescence intensity. The ratio of fluorescence emission was measured at 440 nm with an excitation of 360 nm and curve was fitted by non-linear regression and One-Site specific binding using GraphPad Prism (v6.07). n=3 ± SD.

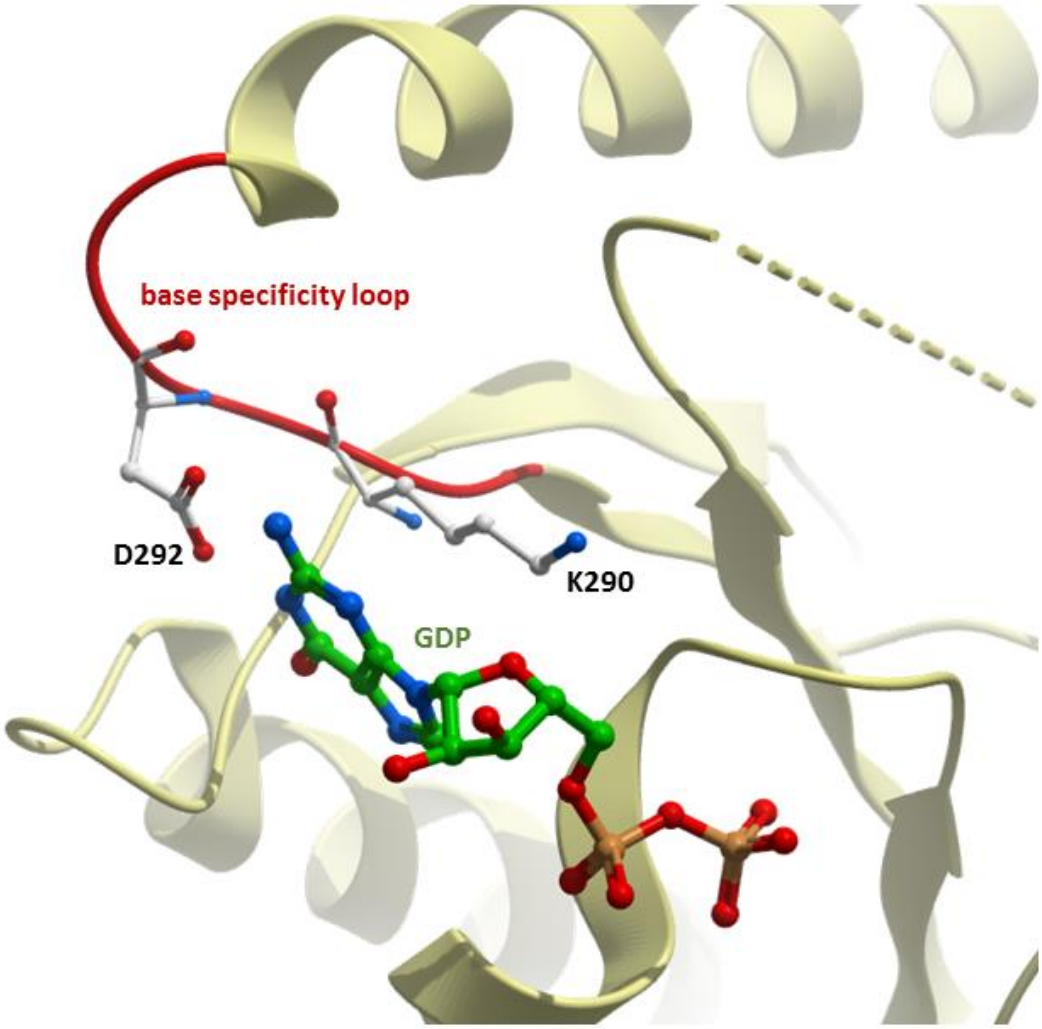

Supp. Figure S2. Role of the base specificity loop in nucleotide binding. The conserved residues Lys290 and Asp292 (white carbon sticks), located in the base specificity loop (red), form direct interactions with a bound GDP (green carbon sticks) in the structure.

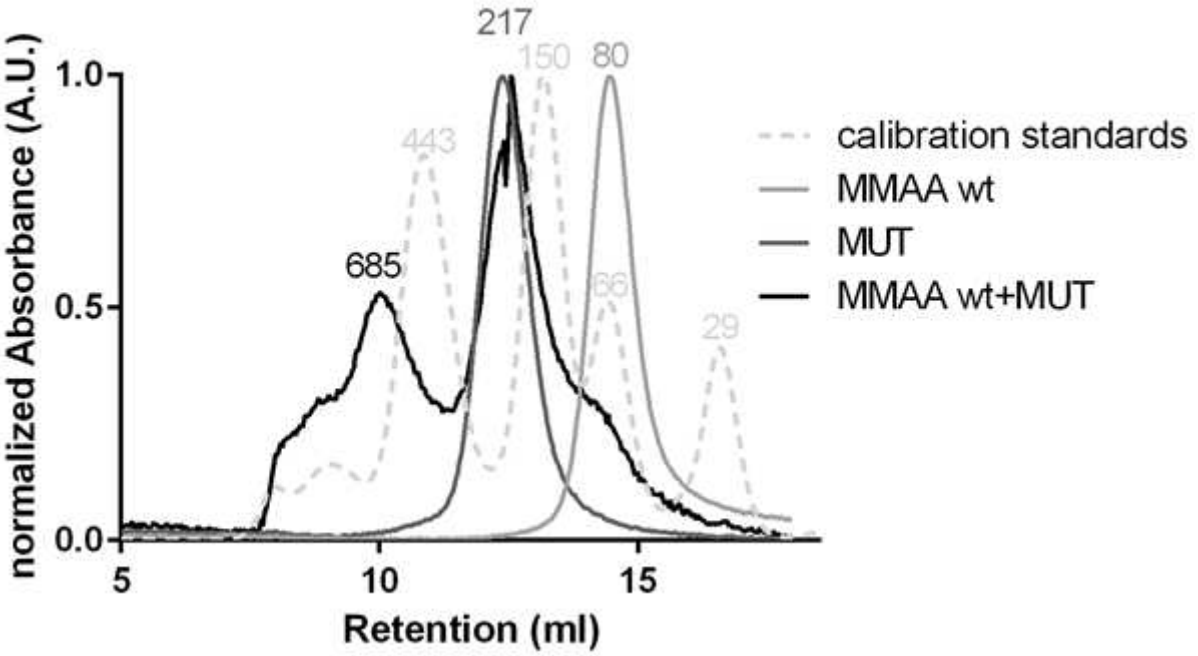

Supp. Figure S3. Gel filtration profiles of calibration standards and MMAA wt and MUT. Calibration of the column was performed using carbonic anhydrase (29 kDa), bovine serum albumin (66 kDa), alcohol dehydrogenase (150 kDa), and apo-ferritin (443 kDa) as MW-standards. Molecular weight of MMAA and MUT was determined by comparing elution volumes with protein standards using the inverse logarithmic relationship between protein size and elution volumes.

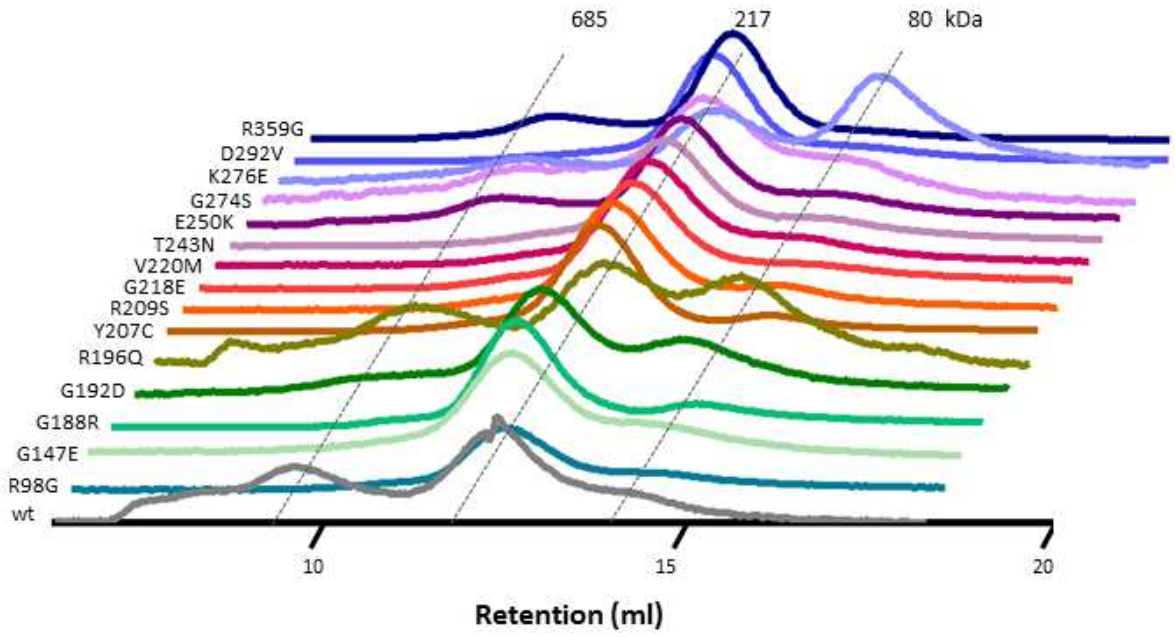

Supp. Figure S4. Analytical gel filtration results of all MMAA mutants analysed on a HiLoad 10/30 Superdex 200 column. Dashed lines indicate the complex peaks (at 685 kDa) as well as individual protein peaks (at 217 kDa: MUT; at 80 kDa: MMAA).

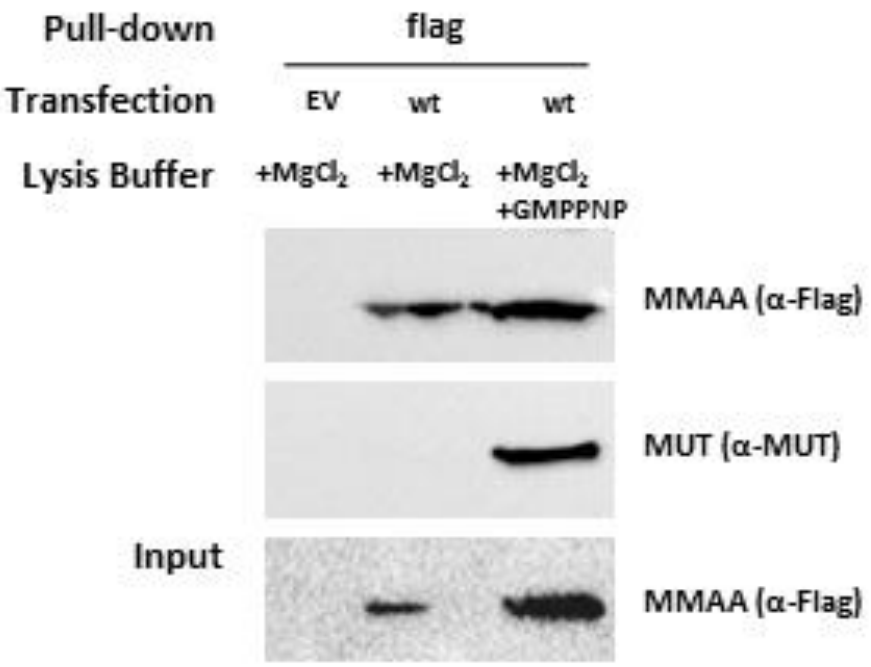

Supp. Figure S5. Interaction of MMAA wt and MUT is dependent on the presence of $MgCl_2$ and GMPPNP. Cell lysates taken from HEK293 cells transfected with either empty vector (EV) or MMAA wt (wt) were supplemented with either 250 µM $MgCl_2$ or 250 µM $MgCl_2$ and 100 µM GMPPNP, then immunoprecipitation using an anti-Flag antibody was performed. Western blot analysis of anti-Flag immunoprecipitates (IP Flag, upper panel) or input lysates (Input, lower panel) with anti-Flag or anti-MUT is shown.

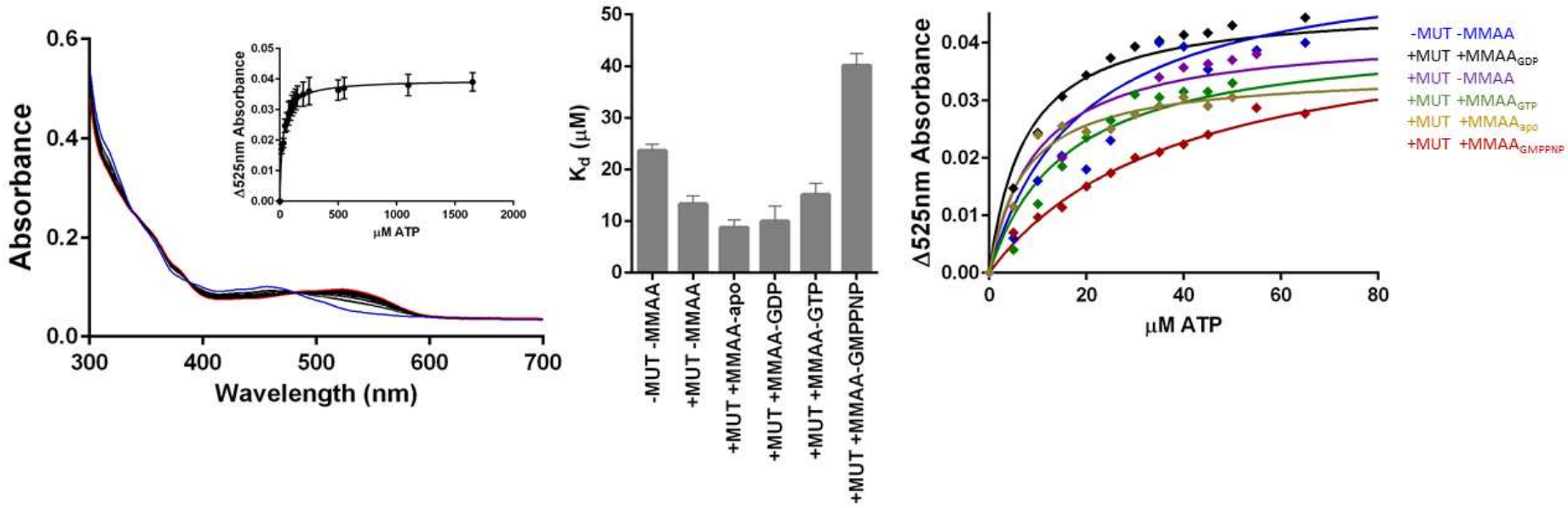

Supp. Figure S6. Release of AdoCbl from MMAB. A: Release of AdoCbl from holo-MMAB (60 μM) after addition of ATP (5-1750 μM) and monitoring the shift in the absorption maxima from 458 nm to 525 nm. Upon ATP addition the absorption maxima changes from 458 nm, depicted in blue, to 525 nm, depicted in red color. Inset: Change in absorption at 525 nm was measured after adding increasing amounts of ATP (5-1750 μM) to 60 μM holo-MMAB. Curve was fitted by non-linear regression and One-Site specific binding using GraphPad Prism (v6.07). n=3 ± SD. **B**: Bargraphs represent K_d values of AdoCbl release from holo-MMAB (60 μM) in the absence or presence of MUT (60 μM) or wt MMAA (60 μM) supplemented with 0.5 mM GDP,GTP or GMPPNP. **C**: Curve-fit of change in absorption at 525 nm generated through release of AdoCbl

from holo-MMAB (60 μM) after the addition of ATP (5-1750 μM) in the absence or presence of MUT (60 μM) or wt MMAA (60 μM) supplemented with 0.5 mM GDP,GTP or GMPPNP. Curve was fitted by non-linear regression and One-Site specific binding using GraphPad Prism (v6.07). n=3, only mean is displayed in graph.

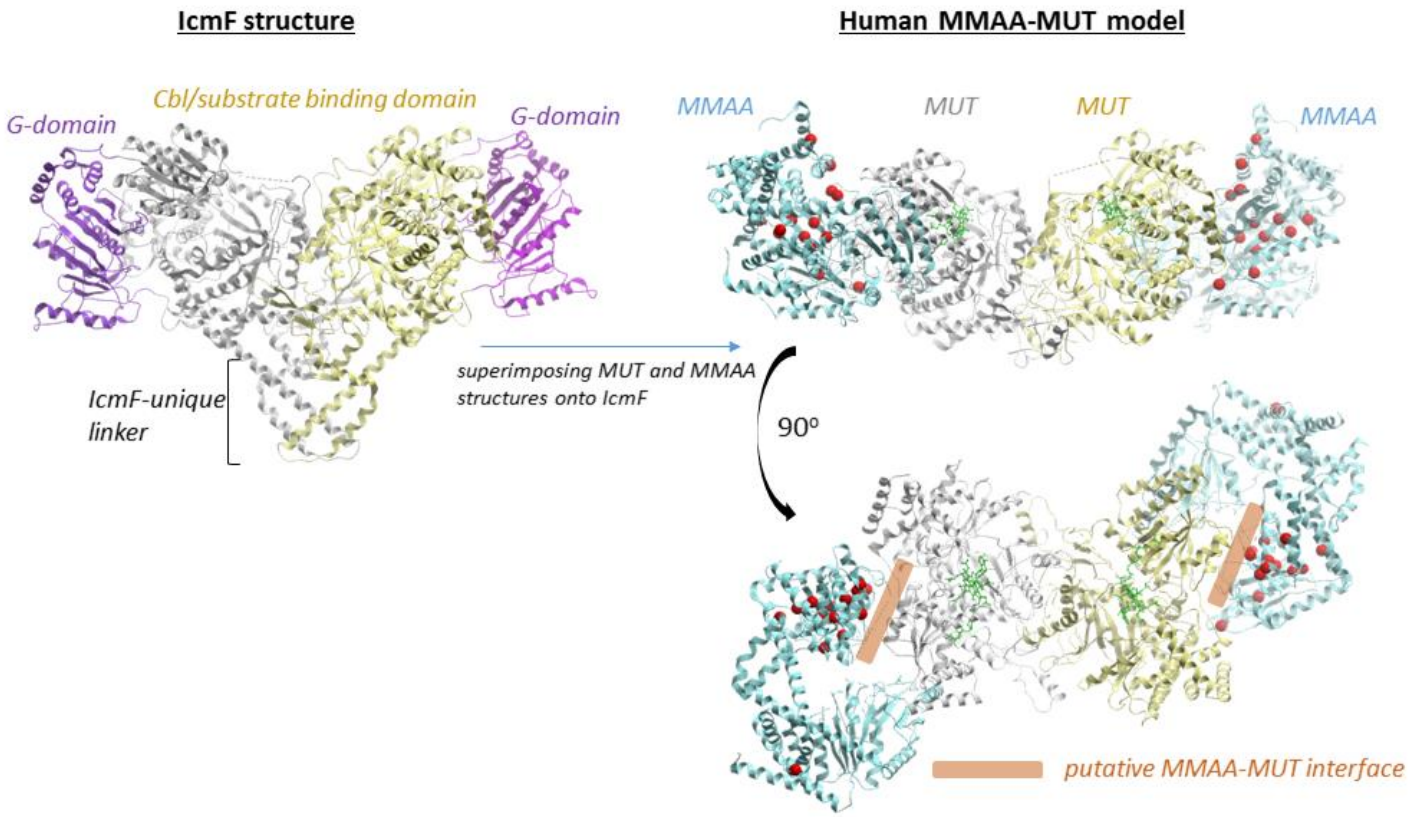

Supp. Figure S7. Modelling of the human MMAA-MUT complex, by superimposing the individual MMAA (PDB 2www) and MUT (PDB 2xiq) structures onto the Cbl/substrate binding domain and G-domain, respectively, of the IcmF 3.25 Å resolution structure (PDB 4xc8).

Supp. Table 1. Overview of all MMAA missense mutations studied.

Patient No.	Mutation 1[a]	predicted change[b]	Mutation 2[a]	predicted change[b]	Reference
WG1449	c.266T>C	p.Leu89Pro	c.64C>T	p.Arg22*	Lerner-Ellis, J.P. et al., 2004
WG2578	c.266T>C	p.Leu89Pro	c.161G>A	p.Trp54*	Lerner-Ellis, J.P. et al., 2005
8	c.292A>G	p.Arg98Gly	c.292A>G	p.Arg98Gly	Vatanavicharn, N. et al., 2012
WG1191	c.434G>A	p.Arg145Gln	c.434G>A	p.Arg145Gln	Lerner-Ellis, J.P. et al., 2004
20	c.434 G>A	p.Arg145Gln	c.433C>T	p.Arg145*	in this study
WG1518	c.440G>A	p.Gly147Glu	c.450_451ins	p.Gly102fs[c]	Lerner-Ellis, J.P. et al., 2004
24	c.562G>C	p.Gly188Arg	c.562G>C	p.Gly188Arg	Merinero, B. et al., 2008
33	c.575G>A	p.Gly192Asp	c.575G>A	p.Gly192Asp	in this study
43	c.[587G>A; 733+1G>A]	p.Arg196Gln/p.?.	c.[587G>A; 733+1G>A]	p.Arg196Gln/p.?.	in this study
WG1943	c.620A>G	p.Tyr207Cys	c.620A>G	p.Tyr207Cys	Lerner-Ellis, J.P. et al., 2004
WG3229	c.627G>T	p.Arg209Ser	c.551dupG	p.Cys184*fs3	Dempsey-Nunez, L. et al., 2012
WG1588	c.653G>A	p.Gly218Glu	c.64C>T	p.Arg22*	Lerner-Ellis, J.P. et al., 2004
54	c.658G>A	p.Val220Met	c.658G>A	p.Val220Met	in this study
55	c.658G>A	p.Val220Met	c.658G>A	p.Val220Met	in this study
51	c.721A>T	p.Ile241Phe	c.592_595delACTG	p.Thr198Serfs*6	in this study
56	c.728C>A	p.Thr243Asn	c.728C>A	p.Thr243Asn	in this study
WG3998	c.748G>A	p.Glu250Lys	c.748G>A	p.Glu250Lys	Dempsey-Nunez, L. et al., 2012
59	c.772G>A	p.Asp258Asn	c.772G>A	p.Asp258Asn	in this study
60	c.772G>A	p.Asp258Asn	c.772G>A	p.Asp258Asn	in this study
WG4075	c.820G>A	p.Gly274Ser	c.820G>A	p.Gly274Ser	Dempsey-Nunez, L. et al., 2012
WG3402	c.826A>G	p.Lys276Glu	mutation not found	-	Dempsey-Nunez, L. et al., 2012
52	c.860C>A	p.Ala287Asp	c.592_595delACTG	p.Thr198Serfs*6	in this study
24	c.875A>T	p.Asp292Val	c.433C>T	p.Arg145*	in this study
7	c.1075C>G	p.Arg359Gly	c.503delC	p.Thr120Metfs[d]	Yang, X. et al., 2004
WG3084	c.1076G>A	p.Arg359Gln	c.433C>T	p.Arg145*	Lerner-Ellis, J.P. et al., 2004
WG2704	c.1076G>A	p.Arg359Gln	c.1076G>A	p.Arg359Gln	Lerner-Ellis, J.P. et al., 2005
42	c.1196_1197delinsTT	p.Gly399Val	c.586C>T	p.Arg196*	in this study

[a] According to NM_172250.2 and NC_000004.12. Nucleotide numbering uses +1 as the A of the ATG translation initiation codon in the reference sequence, with the initiation codon as codon 1.
[b] According to NP_758454.1
[c] frameshift Lerner-Ellis, J.P. et al., 2004

[d] frameshift Yang, X. et al., 2004

Supp. Table 2. AC_{50} and ΔT_m values of MMAA mutants following GDP or GMPPNP binding.

	GDP		GMPPNP	
	AC_{50}	ΔT_m(max)	AC_{50}	ΔT_m(max)
wt	29 ± 3	9.0 ± 0.1	117 ± 32	6.0 ± 0.0
R98G	34 ± 3	9.3 ± 0.4	258 ± 67	6.0 ± 0.2
G147E	22 ± 3	8.7 ± 0.3	115 ± 26	4.6 ± 0.3
G188R	33 ± 5	9.3 ± 0.2	103 ± 23	6.5 ± 0.0
G192D	44 ± 5	9.2 ± 0.3	119 ± 24	6.8 ± 0.2
R196Q	25 ± 5	8.9 ± 0.1	187 ± 48	5.2 ± 0.1
Y207C	35 ± 3	8.9 ± 0.1	269 ± 57	5.7 ± 0.1
R209S	35 ± 4	7.8 ± 0.0	181 ± 41	5.1 ± 0.1
G218E	33 ± 9	8.2 ± 0.5	454 ± 160	4.9 ± 0.1
V220M	35 ± 6	9.1 ± 0.1	218 ± 53	5.8 ± 0.0
T243N	25 ± 3	8.9 ± 0.1	183 ± 51	5.4 ± 0.0
E250K	44 ± 5	9.2 ± 0.3	119 ± 24	6.8 ± 0.2
G274S	34 ± 6	8.7 ± 0.4	247 ± 114	5.3 ± 0.4
K276E	28 ± 4	9.2 ± 0.1	118 ± 25	6.3 ± 0.2
D292V	31 ± 28	1.8 ± 0.1	14 ± 20	1.6 ± 0.1
R359G	28 ± 5	9.5 ± 0.1	196 ± 57	5.9 ± 0.0
K290A+D292A	N.D.	0.8 ± 0.1	N.D.	0.9 ± 0.2

Supp. Table 3. Kinetic parameters of GTP hydrolysis of MMAA mutants.

	Km (μM)	V_{max} (pmol P_i/min)	k_{cat} (min^{-1})	kcat/K_m (min^{-1}/pmol)	Interaction with MUT
wt	42 ± 9	95.8 ± 2.3	0.201 ± 0.005	4.81	yes
R98G	2008 ± 557	46.7 ± 7.5	0.098 ± 0.016	0.049	no
G147E	446 ± 218	98.5 ± 16.3	0.207 ± 0.034	0.463	no
G188R	1430 ± 560	21.6 ± 4.4	0.045 ± 0.009	0.032	no
G192D	178 ± 53	38.4 ± 2.5	0.081 ± 0.005	0.454	yes
R196Q	495 ± 231	70.0 ± 10.9	0.147 ± 0.023	0.297	yes
Y207C	120 ± 53	20.4 ± 1.9	0.043 ± 0.004	0.355	no
R209S	79 ± 39	15.2 ± 1.2	0.032 ± 0.003	0.407	no
G218E	360 ± 147	10.2 ± 1.4	0.021 ± 0.003	0.594	no
V220M	292 ± 75	53.9 ± 3.9	0.113 ± 0.008	0.387	no
T243N	270 ± 135	19.2 ± 2.9	0.040 ± 0.006	0.149	no
E250K	180 ± 61	52.3 ± 4.1	0.110 ± 0.009	0.611	yes
G274S	99 ± 27	35.8 ± 1.7	0.075 ± 0.003	0.759	yes
K276E	124 ± 57	33.3 ± 2.9	0.070 ± 0.006	0.565	yes
D292V	96 ± 33	18.7 ± 1.1	0.039 ± 0.002	0.409	no
R359G	92 ± 25	62.7 ± 3.0	0.131 ± 0.064	1.42	yes